Paper
Int'l J. of Aeronautical & Space Sci. 15(1), 74–81 (2014)
DOI:10.5139/IJASS.2014.15.1.74

IJASS
International Journal of Aeronautical and Space Sciences

Missile two-loop acceleration autopilot design based on $\mathcal{L}_1$ adaptive output feedback control

He Shao-ming* and Lin De-fu**

Beijing Institute of Technology, Beijing, People's Republic of China

Abstract

This article documents the design of a novel two-loop acceleration autopilot based on $\mathcal{L}_1$ adaptive output feedback control for tail-controlled missiles. The inner loop is an adaptive angle-of-attack tracking loop and the outer loop is the traditional PI controller for error compensation. A systematic low-pass filter design procedure is provided for minimum phase system and is applied to the inner loop design while the parameters of the outer loop are obtained from the multi-objective optimization problem. The effectiveness of the proposed autopilot is verified through numerical simulations under various conditions.

Key words: $\mathcal{L}_1$ adaptive output feedback control, Autopilot, low-pass filter

1. Introduction

Due to the wide parameter variation and stringent performance requirements, missile autopilot design is a challenging task. The traditional method of guaranteeing stability in the presence of aerodynamic parameter variation or uncertainty is the gain scheduling control strategy. Modern air-to-air or surface-to-air missiles need large and uncertain flight envelopes, for which accurate aerodynamic parameters are difficult or extremely expensive to obtain from wind tunnel tests; also, the gain scheduling controllers need more operating points. The control objective for these missiles is to ensure accurate interception, with guaranteed robustness, without sacrificing maneuverability. For this purpose, many advanced modern control theories have been extensively studied by numerous researchers to address this problem.

The authors in [1] designed an adaptive angle-of-attack missile autopilot based on Model Reference Adaptive Control (MRAC) and a neural network. However, this scheme cannot compensate for unmatched uncertainties. Some H_∞ design schemes are also offered in [2], but these autopilots may not have satisfactory performance in some operational points, since H_∞ method considers the 'worst case' in the design procedure. In [3], the authors designed a novel dynamic inversion (DI) architecture through output redefinition (i.e., a combination of angle of attack and pitch rate as output instead of the typical acceleration), which they augmented using a neural network. Based on two-time scale separation, the authors in [4] designed a $\mathcal{L}_1$ adaptive state feedback augmented DI autopilot. In [5], the time-delay control and nonlinear observer were adopted for the design of a new angle-of-attack autopilot. Using sliding mode control theory and a PI controller, the authors in [6] designed a two-loop acceleration autopilot, where the inner loop is a sliding mode control (SMC) based angle-of-attack tracking loop and the outer loop is the PI acceleration tracking loop. In [7], adaptive SMC theory is used to design a model-following missile pitch autopilot to reject model uncertainty and disturbance, and the well-known classical PI-type autopilot is constructed as the reference model. In [8], the authors designed a new robust autopilot based on predictive functional control (PFC) to deal with the high nonlinearity of agile missiles while considering the control constraints. A new backstepping autopilot, which guarantees the uniform ultimate boundness, has also been proposed [9]. In [10], the extended observer is utilized to increase the robustness of the input-output linearization based controller

This article considers $\mathcal{L}_1$ adaptive output feedback control

* Graduate Student, Corresponding author: shaoming.he.cn@gmail.com
** Associate Professor

Received: January 8, 2014 Revised : March 7, 2014 Accepted: March 15, 2014

http://ijass.org pISSN: 2093-274x eISSN: 2093-2480

[11, 12], in missile acceleration autopilot design. The key feature of $\mathcal{L}_1$ adaptive control is that it allows fast adaptation without losing robustness. The speed of this architecture is only limited by the available hardware, while robustness is maintained by introducing a low-pass filter. Therefore, this architecture can guarantee transient performance as well as robustness without introducing any high frequency chattering in the control signal in the presence of large adaptation gain. The major difference between output feedback and state feedback [4] architectures is that the uncertainty is not decoupled and enters directly into the underlying transfer functions; therefore, the output feedback scheme has the potential to relax the matching uncertainty assumption. For tail-controlled missiles, the dynamics which describe a missile acceleration are known to be non-minimum phase. Although the $\mathcal{L}_1$ adaptive output feedback controller can be applied to these systems, the low-pass filter and reference model selection that satisfy the closed-loop stability criteria are quite limited and the performance cannot be guaranteed. In order to avoid this problem, we presented a two-loop architecture autopilot, which contains an adaptive angle-of-attack tracking inner loop and an acceleration tracking outer loop. For the inner loop, a systematic low-pass filter design procedure is provided. The stability of the $\mathcal{L}_1$ adaptive controller is verified through Kharitonov theorem. For the outer loop, the traditional PI controller is introduced to compensate the acceleration error. The simulation results under various conditions show that the proposed autopilot is more advantageous in the presence of external time-varying disturbances.

This paper is organized as follows. Sec. 2 provides the missile model and some preliminaries of $\mathcal{L}_1$ adaptive control. A systematic low-pass filter procedure is presented in Sec. 3. Sec. 4 gives the details of the autopilot design process while Sec. 5 shows some numerical simulations. Finally, some conclusions are offered in Sec. 6.

2. Problem Formulation

2.1 Missile Model

For tail-controlled, aerodynamic symmetrical, skid-to-turn, cruciform-type missiles, under the small perturbation assumption, their pitch channel equations can be formulated as [13]:

$$\begin{aligned}
&\dot{\alpha} = \dot{\vartheta} - b_\alpha \alpha - b_\delta \delta \\
&\ddot{\vartheta} = -a_\omega \dot{\vartheta} - a_\alpha \alpha - a_\delta \delta \\
&\alpha = \vartheta - \gamma \\
&a_y = V\dot{\gamma}
\end{aligned} \tag{1}$$

where α denotes the angle-of-attack, ϑ the body pitch angle, γ the flight path angle, δ the actuator deflection angle, and a_y the missile lateral acceleration; the definitions of aerodynamic coefficients can be seen in [13].

2.2 Preliminaries of $\mathcal{L}_1$ Output Feedback Control

Consider the following single-input-single-output (SISO) system:

$$y(s) = A(s)\left(u(s) + d(s)\right) \tag{2}$$

where $y(s)$ and $u(s)$ are the Laplace transforms of the system's output and input signals, respectively, $A(s)$ is a strictly proper unknown transfer function with a known relative degree, $d(s)$ is the Laplace transform of the time-varying uncertainties $d(t)=f(t, y(t))$, for which there are constants and L, L_0, L_1, L_2, L_3, such that

$$\begin{aligned}
&\left|f(t,y_1) - f(t,y_2)\right| \le L\left|y_1 - y_2\right| \\
&\left|f(t,y)\right| \le L\left|y\right| + L_0 \qquad , \qquad \forall t \in R^+ \\
&\left|\dot{d}(t)\right| \le L_1\left|\dot{y}(t)\right| + L_2\left|y(t)\right| + L_3
\end{aligned} \tag{3}$$

The control objective is to find a control law such that $y(s) \approx M(s)u(s)$, where $M(s)$ denotes the reference model. Note that the system in (1) can be rewritten in terms of the reference model

$$y(s) = M(s)\left(u(s) + \sigma(s)\right) \tag{4}$$

where $\sigma(s)=[(A(s)-M(s))u(s)+A(s)d(s)]/M(s)$. Let $\left(A_m, b_m, c_m^T\right)$ be the minimum realization of $M(s)$. Further, since A_m is a Hurwitz matrix, $P=P^T>0$ exists and is the solution of the following Lyapunov function

$$A_m^T P + PA_m = -Q\,,\ \ Q = Q^T > 0 \tag{5}$$

Since P is positive definitive, P can be rewritten as $P = \left(\sqrt{P}\right)^T \sqrt{P}$, where $\sqrt{P}$ is non-singular. Let D contain the null space of $c_m^T\left(\sqrt{P}\right)^{-1}$, i.e., $D\left(c_m^T\left(\sqrt{P}\right)^{-1}\right) = 0$, and further let $\Lambda \triangleq \left[c_m \quad \left(D\sqrt{P}\right)^T\right]^T$. Finally, let T_s be the sample rate of the control system, and $\mathrm{I}_1 \triangleq [1, 0, \ldots, 0]^T$. Then, the $\mathcal{L}_1$ adaptive output feedback controller is introduced as follows:

The state-predictor is given by

$$\begin{aligned}
&\dot{\hat{x}} = A_m\hat{x} + b_m u(t) + \hat{\sigma}(t) \\
&\hat{y}(t) = c_m^T\hat{x}(t)
\end{aligned} \tag{6}$$

where $\hat{\sigma}(t)$ is the adaptive parameter, which is determined by the following adaptive law:

$$\hat{\sigma}(t) = -\Phi^{-1}(T_s)\mu(iT_s) \quad , t \in \left[iT_s, (i+1)T_s\right] \tag{7}$$

where $i = 0,1,2,\ldots$, $\tilde{y} \triangleq \hat{y}(t) - y(t)$, and

$$\begin{aligned} &\Phi(T_s) \triangleq \Lambda A_m^{-1}\left(I - e^{A_m(T_s-\tau)}\right) \\ &\mu(iT_s) \triangleq e^{\Lambda A_m A^{-1} T_s} \mathrm{I}_1 \tilde{y}(iT_s) \end{aligned} \quad , i = 0,1,2,\ldots \tag{8}$$

The control law is defined as:

$$u(s) = C(s)r(s) - \frac{C(s)c_m^T(sI - A_m)^{-1}}{c_m^T(sI - A_m)^{-1}b_m}\hat{\sigma}(s) \tag{9}$$

where $r(s)$ is the Laplace transform of the reference command, and $C(s)$ is a stable strictly-proper low-pass filter, which has unit DC gain, i.e., $C(0)=1$.

For stability, the selection of $C(s)$ and $M(s)$ must ensure that

$$H(s) = \frac{A(s)M(s)}{C(s)A(s) + (1 - C(s))M(s)} \tag{10}$$

is stable and the following $\mathcal{L}_1$-norm condition holds

$$\left\| G(s) \right\|_{\mathcal{L}_1} L < 1 \tag{11}$$

where $G(s)=H(s)(1-C(s))$.

In order to evaluate the performance of the closed-loop, consider the following non-adaptive ideal reference system:

$$\begin{aligned} y_{ref}(s) &= M(s)\left(u_{ref}(s) + \sigma_{ref}(s)\right) \\ u_{ref}(s) &= C(s)\left(r(s) - \sigma_{ref}(s)\right) \end{aligned} \tag{12}$$

where $\sigma_{ref}(s)=[(A(s)-M(s))u_{ref}(s)+A(s)d_{ref}(s)]/M(s)$ and $d_{ref}(s)$ is the Laplace transform of $f(t, y_{ref}(t))$. The performance bounds of the $\mathcal{L}_1$ adaptive output feedback controller are summarized in the following Lemma.

Lemma 1 [11]. Consider the uncertain system (2) and the adaptive controllers (6), (7), and (8) subject to conditions (10) and (11). If we choose

$$\gamma_0(T_s) < \overline{\gamma}_0 \tag{13}$$

where $\gamma_0(T_s)$ is a computable bound and $\overline{\gamma}_0$ is an arbitrarily positive constant, then

$$\begin{aligned} &\left\| \tilde{y} \right\|_{\mathcal{L}_\infty} < \overline{\gamma}_0 \\ &\left\| y_{ref} - y \right\|_{\mathcal{L}_\infty} < \gamma_1(T_s) \\ &\left\| u_{ref} - u \right\|_{\mathcal{L}_\infty} < \gamma_2(T_s) \end{aligned} \tag{14}$$

where $\gamma_1(T_s)$ and $\gamma_2(T_s)$ are computable bounds that can be reduced to arbitrarily small sizes by decreasing the sampling time T_s.

3. Low-pass Filter Design

Substituting the expression of $\sigma_{ref}(s)$ into $y_{ref}(s)$ in Eq. 12 gives

$$\begin{aligned} y_{ref}(s) &= M(s)\left(u_{ref}(s) + \sigma_{ref}(s)\right) \\ &= M(s)\left(u_{ref}(s) + \frac{(A(s) - M(s))u_{ref}(s) + A(s)d_{ref}(s)}{M(s)}\right) \\ &= A(s)\left(u_{ref}(s) + d_{ref}(s)\right) \end{aligned} \tag{15}$$

Substituting the expression of $\sigma_{ref}(s)$ into $u_{ref}(s)$ in Eq. 12 gives

$$\begin{aligned} u_{ref}(s) &= C(s)\left(r(s) - \sigma_{ref}(s)\right) \\ &= C(s)\left(r(s) - \frac{(A(s) - M(s))u_{ref}(s) + A(s)d_{ref}(s)}{M(s)}\right) \\ &= C(s)r(s) - \frac{C(s)(A(s) - M(s))}{M(s)}u_{ref}(s) - \frac{C(s)A(s)}{M(s)}d_{ref}(s) \end{aligned} \tag{16}$$

Solving Eq. 15 for $u_{ref}(s)$ yields

$$u_{ref}(s) = \frac{C(s)M(s)r(s) - C(s)A(s)d_{ref}(s)}{C(s)A(s) + (1 - C(s))M(s)} \tag{17}$$

Substituting the expression of $u_{ref}(s)$ into $y_{ref}(s)$ in Eq. 15 gives

$$\begin{aligned} y_{ref}(s) &= A(s)\left(\frac{C(s)M(s)r(s) - C(s)A(s)d_{ref}(s)}{C(s)A(s) + (1 - C(s))M(s)} + d_{ref}(s)\right) \\ &= A(s)M(s)\left(\frac{C(s)r(s) + (1 - C(s))d_{ref}(s)}{C(s)A(s) + (1 - C(s))M(s)}\right) \\ &= \frac{A(s)M(s)}{C(s)A(s) + (1 - C(s))M(s)}\left(C(s)r(s) + (1 - C(s))d_{ref}(s)\right) \\ &= H(s)\left(C(s)r(s) + (1 - C(s))d_{ref}(s)\right) \end{aligned} \tag{18}$$

Consider the following general form of a low-pass filter:

$$C(s) = \frac{b_k(\tau s)^k + b_{k-1}(\tau s)^{k-1} + \cdots + b_0}{(\tau s)^l + a_{l-1}(\tau s)^{l-1} + \cdots + a_1(\tau s) + a_0} \tag{19}$$

where $\tau>0$ is the time constant of the low-pass filter; k, l are positive integers subject to $1-k>0$; and $a_0=b_0$.

From Eq. 18, it can be found that $\left\| H(s)(1 - C(s)) \right\|_{\mathcal{L}_1}$ should be minimized for disturbance rejection. Also, from the form of Eq. 19, one can imply that

$$\lim_{\tau \to 0} \left\| H(s)(1 - C(s)) \right\|_{\mathcal{L}_1} = 0 \tag{20}$$

In [14], the authors reveal that the architecture of the $\mathcal{L}_1$ adaptive output feedback control is equivalent to that of the disturbance observer (DOB). Therefore, the necessary and

sufficient robust stability criteria of DOB in [15] can be applied to the low-pass filter desi gn of the $\mathcal{L}_1$ adaptive output feedback control, which is summarized in the following lemma.

Lemma 2. Let $A(s)$ belong to the following transfer function set:

$$\mathcal{P}=\left\{P(s)=\frac{\beta_{n-r}s^{n-r}+\beta_{n-r-1}s^{n-r-1}+\mathrm{L}+\beta_0}{\alpha_n s^n+\alpha_{n-1}s^{n-1}+\mathrm{L}+\alpha_0}\middle|\alpha_i\in[\alpha_{li},\alpha_{ui}],\beta_i\in[\beta_{li},\beta_{ui}]\right\} \quad (21)$$

where n, r are positive integers and α_{li}, α_{ui}, β_{li}, β_{ui} are known constants that satisfy $0\notin[\alpha_{li},\alpha_{ui}]$ and $0\notin[\beta_{li},\beta_{ui}]$. A constant $\tau^*>0$ exists such that for all $0<\tau\le\tau^*$, $H(s)$ is stable if the following two conditions hold:

i) $M(s)$ and $A(s)\in\mathcal{P}$ are minimum phases and have the same relative degree;

ii) $p_f(s)=C_d(s;1)+\left(\lim_{s\to\infty}\frac{A(s)}{M(s)}-1\right)C_n(s;1)$ is a Hurwitz equation for all $A(s)\in\mathcal{P}$.

where $C_d(s;1)$ and $C_n(s;1)$ denote the denominator and the numerator of the low-pass filter for τ=1, respectively.

Proof. See the proof of Theorem 3 in [15].

From Eq. 19 and Lemma 2, one can imply that a positive constant $\tau_0\le\tau^*$ always exists, such that condition (11) holds. In order to compute the exact value of τ_0, we introduced the well-known Kharitonov theorem:

Lemma 3 [16]. The polynomial family

$$P(s,\mathcal{I}_a)=\left\{p(s,a)=\sum_{i=0}^{n}a_i s^i : a\in\mathcal{I}_a\right\}, a_n>0 \text{ is stable only}$$

if the following four polynomials are stable:

$$\begin{aligned}
\kappa_1&=a_{u0}+a_{l1}s+a_{l2}s^2+a_{u3}s^3+a_{u4}s^4+\cdots,\\
\kappa_2&=a_{u0}+a_{u1}s+a_{l2}s^2+a_{l3}s^3+a_{u4}s^4+\cdots,\\
\kappa_3&=a_{l0}+a_{u1}s+a_{u2}s^2+a_{l3}s^3+a_{l4}s^4+\cdots,\\
\kappa_4&=a_{l0}+a_{l1}s+a_{u2}s^2+a_{u3}s^3+a_{l4}s^4+\cdots,
\end{aligned} \quad (22)$$

where $\mathcal{I}_a\triangleq\{a_i\in[a_{li},a_{ui}],i=1,\ldots,n\}$.

Based on the above analysis, the systematic low-pass filter design procedure is summarized as:

Step 1: Choosing a possible candidate low-pass filter and checking the Hurwitz condition of $p_f(s)$;

Step 2: Using Lemma 3 and MATLAB polynomial toolbox [17] to calculate the value of τ^*;

Step 3: Decreasing τ from τ^* to obtain the exact value of τ_0 such that condition (11) holds.

4. Autopilot Design

For tail-controlled missiles, the transfer function from fin deflection to lateral acceleration has right-half-plane (RHP) zeros; thus, it is a non-minimum phase system and the condition i) in Lemma 2 is violated. Therefore, in order to use the above procedure to design the missile acceleration autopilot, a novel two-loop autopilot architecture which has a $\mathcal{L}_1$ angle-of-attack tracking inner loop and a PI outer loop is introduced. The block is shown in Fig. 1.

4.1 Inner Loop Design

Assumption 1. For angle-of-attack tracking, we omit the term $b_\delta\delta$ in equation (32). Note that, in most cases, the actuator deflection is used to produce a moment to control the missile attitude, hence $b_\delta\delta$ is very small [10, 13].

After some algebra calculations, we have

$$\frac{\alpha(s)}{\delta(s)}=\frac{-a_\delta}{s^2+(a_\omega+b_\alpha)s+a_\alpha+a_\omega b_\alpha} \quad (23)$$

The reference model for angle-of-attack tracking is selected as

$$M(s)=\frac{1}{\left(\frac{s}{\omega_m}\right)^2+\frac{2\xi_m}{\omega_m}s+1} \quad (24)$$

where the natural frequency and damping ratio are set as 8π and 0.707, respectively.

The low-pass filter is selected as

$$C(s)=\frac{1}{(\tau s)^2+2\alpha\tau s+1} \quad (25)$$

where τ and α are the two tuning parameters. Note that a more complex low-pass filter can be chosen to improve the closed-loop performance, which is an open problem.

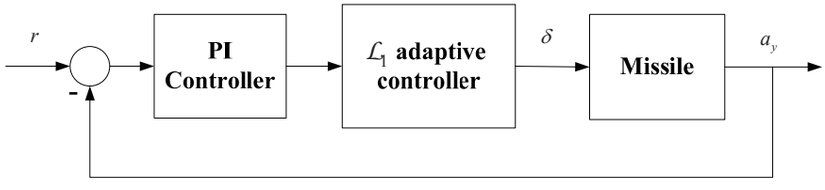

Fig. 1. Architecture of the proposed autopilot

4.2 Outer Loop Design

Although the exact relation between angle-of-attack and lateral acceleration can be derived, the exact missile model is difficult to obtain. In order to compensate the acceleration errors, the traditional PI controller in conjunction with Particle Swarm optimization (PSO) algorithms [18] is adopted, where the cost function is selected as

$$J = k_1 \left| \frac{t_s - t_{sd}}{t_{sd}} \right| + k_2 \left| \text{overshoot} \right| + k_3 \left| \frac{a_y - r}{r} \right| \tag{26}$$

where k_1, k_2, k_3>0, such that k_1+k_2+k_3=0, t_s denotes the settling time and t_{sd} denotes the desired settling time.

5. Simulation Results

In this section, the performance of the proposed adaptive autopilot is verified via numerical simulations. The missile aerodynamic parameters are taken from [19] and are b_α=1.6, b_δ=0.23, a_α=250, a_δ=280 and a_ω=1.5. The scaling factors in the cost function are selected as k_1=0.2, k_2=0.6, k_3=0.2 and the sampling time T_s is set as 0.001s. Based on the design procedure given in Sec. 3 and the multi-objective optimization problem presented in Sec. 4.2, the low-pass filter and PI controller are obtained as:

$$C(s) = \frac{1}{\left(\frac{s}{250}\right)^2 + \frac{1.582}{250}s + 1}, \; K_p = 1.417 \times 10^{-5}, \; K_I = 0.003871 \tag{27}$$

where K_p and K_I denote the proportional constant and integral constant, respectively.

5.1 Inner Loop Performance

First, the effectiveness of the inner angle-of-attack tracking loop is demonstrated in the presence of aerodynamic parameter uncertainty. The angle-of-attack response and control effort are plotted in Figs. 2 and 3, respectively, where K denotes +K perturbation in a_α, b_α, and a_ω, and –K perturbation in a_δ and b_δ. These figures show that the proposed inner loop has a satisfactory tracking performance in the presence of model uncertainties.

Next, the simulations are carried out in the presence of nonlinear disturbances, wherein the following form of disturbance is selected:

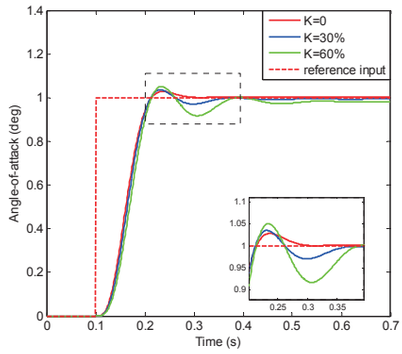

Fig. 2. Angle-of-attack response

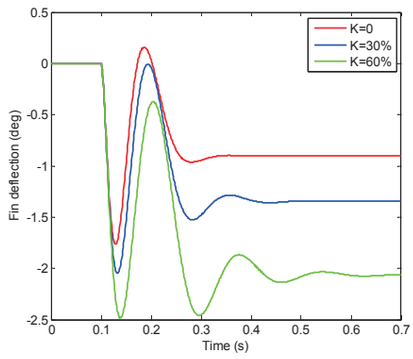

Fig. 3. Control effort

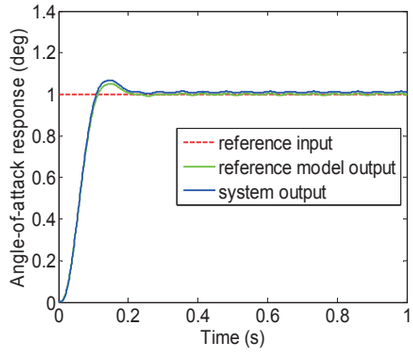

Fig. 4. Angle-of-attack response

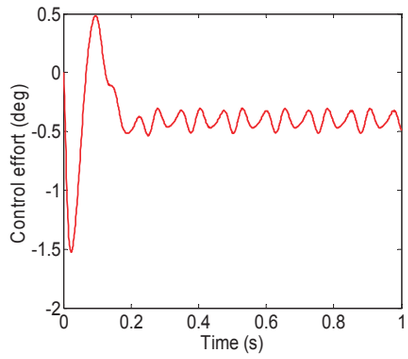

Fig. 5. Control effort

$$d(t)=\left[0.1\sin(100t)+0.05\sin(150t)+0.5y(t)\right]\text{deg} \tag{28}$$

Figs. 4 and 5 present the angle-of-attack response and control effort profiles, respectively. It can be seen that the fast adaptation of the $\mathcal{L}_1$ adaptive controller guarantees smooth and uniform transient performance in the presence of time-varying disturbance. Furthermore, the frequency in the control signal matches the frequency of the selected time-varying disturbance for which the controller is intended to compensate.

Finally, the effects of sampling rate and bandwidth of the low-pass filter on the closed-loop performance are investigated. Figs. 6 and 7 present the angle-of-attack response and tracking error for different sampling rates. It can be seen that the tracking error can be reduced by decreasing the sampling rate if hardware is available. However, the improvement of the tracking error is very limited when the sampling rate is less than 0.001s; therefore, 0.001s is selected in the above simulations. Then, another low-pass filter is selected as:

$$C_1(s)=\frac{1}{\left(\frac{s}{120}\right)^2+\frac{1.4}{120}s+1} \tag{29}$$

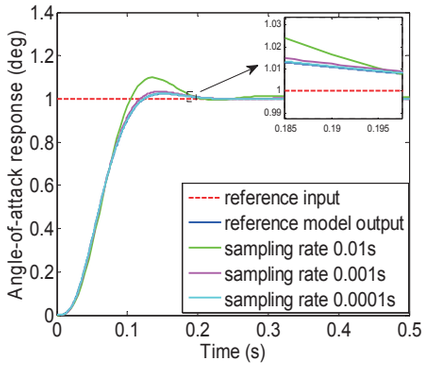

Fig. 6. Angle-of-attack response

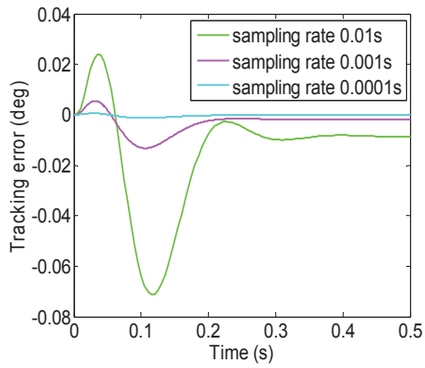

Fig. 7. Tracking error

Figs. 8 and 9 give the bode diagram and the angle-of-attack response in both low-pass filters. It can be seen that the closed-loop performance under $C(s)$ is superior. Since the bandwidth of $C(s)$ is larger than that of $C_1(s)$, more errors can be canceled out. However, if the chosen bandwidth of the low-pass filter is too small, the robustness of the closed loop adaptive controller will reduce significantly.

5.2 Outer Loop Performance

In order to investigate the performance of the proposed autopilot, some comparisons with the classical three-loop autopilot [20] are made in this part, where the parameters of the three-loop autopilot are selected as: time constant 0.2s, second order damping ratio 0.9, and crossover frequency 45rad/s.

Figs. 10 and 11 provide the acceleration response for both autopilots in the nominal case and in the presence of time-varying disturbance and 20% aerodynamic parameter uncertainty, respectively, where the time-varying disturbance is chosen arbitrarily as:

$$d(t)=\left[0.5\sin(100t)+0.3\sin(150t)\right]\text{deg} \tag{30}$$

As shown in these two figures, both autopilots show satisfactory performance in the nominal case, and the

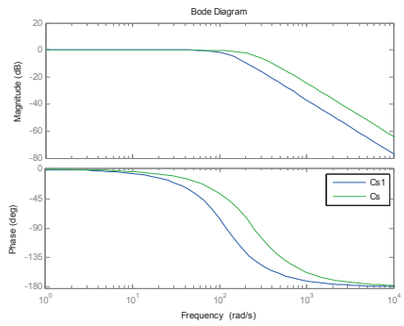

Fig. 8. Bode diagram

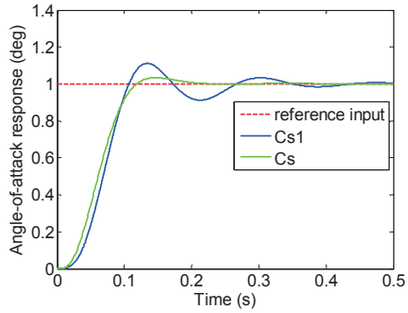

Fig. 9. Angle-of-attack response

$\mathcal{L}_1$ adaptive autopilot shows nearly the same response as that in the nominal case while the classical three-loop autopilot, not surprisingly, shows a different response since, unlike the adaptive autopilot, the classical three-loop autopilot does not have an estimation loop to estimate the external disturbance. Note that $d(t)$ is only restricted in the Lipschitz norm; therefore, the $\mathcal{L}_1$ adaptive autopilot is more advantageous in the presence of actuator failures and other exogenous disturbances.

6. Conclusion

This paper considers $\mathcal{L}_1$ adaptive output feedback control theory to the application of autopilot design for tail-controlled missiles. The proposed architecture has two loops: the inner loop is an adaptive angle-of-attack tracking loop and the outer loop is the traditional PI controller loop. Numerical simulation results show that the $\mathcal{L}_1$ adaptive autopilot is more advantageous in the presence of time-varying disturbances. However, since the closed-loop adaptive system is nonlinear and time-varying, classical stability criteria such as a phase margin cannot be applied to the stability analysis. Although some time-delay margin calculation algorithms exist [21-23], many of these are conservative and the exact value of time-delay is difficult to calculate, which is the main limit for the practical application of adaptive control.

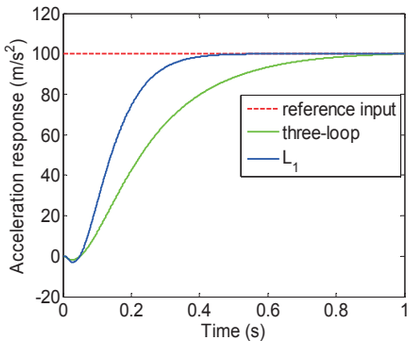

Fig. 10. Acceleration response

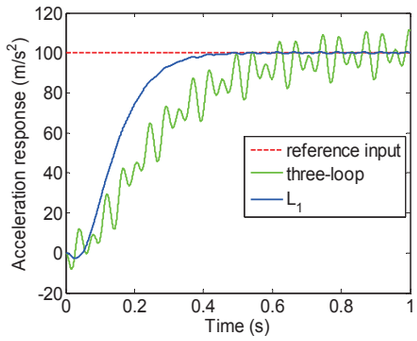

Fig. 11. Acceleration response

Acknowledgement

The authors are grateful to Prof. Chengyu Cao and Dr. Luo Jie from the University of Connecticut for their thoughtful discussions of $\mathcal{L}_1$ adaptive control theory. Finally the authors are grateful to the editor and the anonymous reviewers for their helpful comments and constructive suggestions with regard to the revision of the paper.

References

[1] Wise, Kevin A., "Robust stability analysis of adaptive missile autopilots", *AIAA Paper*, 2008-6999, 2008, pp. 18-21.

[2] Wise, Kevin A., "A trade study on missile autopilot design using optimal control theory", *Proceedings of the 2007 AIAA Guidance, Navigation, and Control Conference*, Hilton Head, USA, 2007.

[3] Sharma, M., Calise, A. J., and Corban, J. E., "Application of an adaptive autopilot design to a family of guided munitions", *Proceedings of the 2000 AIAA Guidance, Navigation, and Control Conference*. Denver, USA, 2000.

[4] Peter, F., Holzapfel, F., Xargay, E., and Hovakimyan, N., "L1 Adaptive Augmentation of a Missile Autopilot", *Proceedings of the 2012 AIAA Guidance, Navigation, and Control Conference*. Minnesota, USA, 2012.

[5] C. H, Lee., T. H., Kim., and M. J. Tahk., "Missile autopilot design for agile turn using time delay control with nonlinear observer", *International Journal of Aeronautical and Space Science and Technology*, Vol. 12, No.3, 2011, pp. 266-273.

[6] Kim, S. H., and M. J. Tahk., "Missile acceleration controller design using proportional–integral and non-linear dynamic control design method", *Proceedings of the Institution of Mechanical Engineers, Part G: Journal of Aerospace Engineering*, Vol. 226, No. 8, 2012, pp. 882-897.

[7] Choe, D. G., and Kim, J. H. "Pitch autopilot design using model-following adaptive sliding mode control". *Journal of Guidance, Control, and Dynamics*, Vol. 25, No. 4, 2002, pp. 826-829.

[8] Tang, W. Q., and Cai, Y. L., "Predictive Functional Control Based Missile Autopilot Design". *Journal of Guidance, Control, and Dynamics*, Vol. 35, No. 5, 2012, pp. 1450-1455.

[9] Kim, S. H., Kim, Y. S., and Song, C., "A robust adaptive nonlinear control approach to missile autopilot design". *Control engineering practice*, Vol. 12, No. 2, 2004, pp. 149-154.

[10] Godbole, A. A., T. R. Libin, and S. E. Talole., "Extended

state observer-based robust pitch autopilot design for tactical missiles." *Proceedings of the Institution of Mechanical Engineers, Part G: Journal of Aerospace Engineering*, Vol. 226, No. 12, 2012, pp. 1482-1501.

[11] Cao, C., and Hovakimyan, N., "L1 adaptive output-feedback controller for non-strictly-positive-real reference systems: missile longitudinal autopilot design", *Journal of Guidance, Control, and Dynamics*, Vol. 32, No. 3, 2009, pp. 717-726.

[12] Hovakimyan, N., and Cao, C., L1 *Adaptive Control Theory: Guaranteed Robustness with Fast Adaptation*. Vol. 21. Siam, Philadephia, 2010.

[13] Garnell P. *Guided Weapon Control System*, 2nd ed., Pergamon , New York, 1980

[14] Kharisov, E., Kim, K. K. K., Wang, X., and Hovakimyan, N., "Limiting behavior of L1 adaptive controllers." *Proceedings of AIAA Guidance, Navigation and Control Conference*, Portland, OR. 2011.

[15] Hyungbo Shim., and Nam H. Jo., "An almost necessary and sufficient condition for robust stability of closed-loop systems with disturbance observer." *Automatica*, Vol. 45, No. 1, 2009, pp. 296-299.

[16] Bhattacharyya, S. P., H. Chapellat, and L. H. Keel,. *Robust control*, Prentice-Hall, Upper Saddle River, New Jersey, 1995.

[17] PolyX, Ltd, *The Polynomial Toolbox for MATLAB® Manual*. 1999

[18] Kennedy, J., and Eberhart, R,. Particle swarm optimization. *Proceedings of IEEE international conference on neural networks*, Vol. 4, No. 2, 1995, pp. 1942-1948.

[19] Nesline, F. William, and Mark L. Nesline., "How autopilot requirements constrain the aerodynamic design of homing missiles", *Proceedings of the 1984 American Control Conference*, IEEE, San Diego, USA, 1984.

[20] Zarchan P., *Tactical and strategic missile guidance*, 3rd ed., AIAA, Washington, DC, 1998.

[21] Annaswamy, A., Jang, J., and Lavretsky, E., "Stability Margins for Adaptive Controllers in the Presence of Time Delay," *AIAA Guidance, Navigation, and Control Conference*, Honolulu, USA, 2008.

[22] Nguyen, N., and Summers, E.,"On Time Delay Margin Estimation for Adaptive Control and Robust Modification Adaptive Laws." *AIAA Guidance, Navigation, and Control Conference*, Portland, USA, 2011.

[23] Dorobantu, A., Seiler, P., and Balas, G. J., "Time-delay margin analysis for an adaptive controller." *Journal of Guidance, Control, and Dynamics*, Vol. 35, No. 5, 2012, pp. 1418- 1425